OPERATING PRINCIPLE AND ANALYTICAL FUNDAMENTALS*

**OPERATING PRINCIPLE AND ANALYTICAL FUNDAMENTALS**

2.1.   Introduction

High power microwave (HPM) sources are required for various applications, such as, directed energy weapons, electronic warfare, EMP and HPEM simulators, etc. Reltron is one of the potential sources for such applications. The existing high peak power HPM sources, such as, MILO suffers from the problem of pulse shortening, above the pulse duration of 35-40 ns, while reltron can provide pulse power of more than 100 ns duration. Vircator is also a dominant HPM sources, however, due to its lower efficiency; it is not found useful for the HPM systems. The electronic efficiency of the reltron is approximately 50% in the lower microwave frequency bands. Its other merits, such as, repetitive pulse operation, frequency agility, direct RF power extraction without mode converter and compactness, make this device a strong competitor as an HPM source over the other relativistic devices of the klystron and magnetron families [Benford *et al.* (2007)]. In 1992, the first experimental reltron was developed at M/s Titan Spectron, US [Miller *et al.* (1992)]. Later, an analytical model of the rectangular output section was provided to determine the cavity and iris dimensions to optimize RF output power [Miller *et al.* (1994)]. In 1997, using split cavity oscillator [Marder *et al.* (1992)] a physical description of the RF signal growth and the analysis for the beam bunching in the modulation cavity as well as pre-bunched beam radiation in the output cavity was demonstrated [Ding (1997)]. In 2012, some modifications were proposed in the reltron which utilizes multiple modes to increase the RF output power and developed an analytical model taking beam modulation coefficient into consideration [Soh *et al.* (2012)].
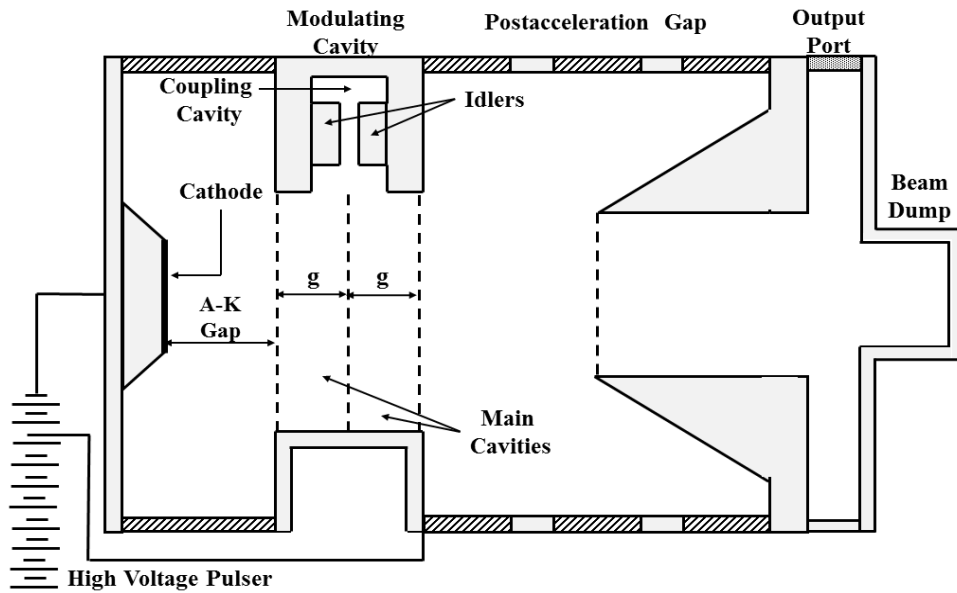
Figure 2.1: Schematic diagram of a reltron.

In the present chapter, with the help of a typical schematic diagram of the reltron, the operating principle of the device is presented along with brief description of the each subassemblies. The analytical fundamentals of the device, such as, sustained oscillation condition and electronic efficiency of the device is described using mathematical modeling and the analytical results obtained are also validated through the published experimental values.

2.2. Reltron Device Description

Reltron is a slow wave microwave oscillator capable of generating hundreds of megawatt (MW) pulse power in the frequency range of 0.5 – 12 GHz. The self-magnetic insulating behaviour of the device eliminates the need of the external DC magnetic field. This device also meets the necessary conditions required for an efficient HPM source, such as, highly bunched electron beam; less electron energy spread and efficient energy extraction without RF breakdown [Miller *et al.* (1992)]. Post-acceleration and the multi-cavity output sections are the vital subassemblies of the

reltron [Marder *et al.* (1992)]. The principal operating mode of the device is TM_{01}. This device has an additional advantage of the direct RF output extraction through a rectangular waveguide in its fundamental TE_{10} mode without any mode converter [Miller *et al.* (1992)].

2.2.1. Reltron Components

A typical schematic of the reltron oscillator is shown in Fig. 2.1, which consists of a high voltage pulser, field emissive cathode, modulation cavity, post-acceleration gap, RF extraction cavity and a beam dump [Miller *et al.* (1992)].

(a)   DC Power Supply

Several high voltage sources have been used to drive the reltron. Initially, it has been operated with Marx generator with a crowbar switch to precisely control the pulse duration. For applications requiring repetition rates upto a few tens of Hertz PFN Marx pulsers are used while the applications requiring repetition rate in excess of few tens of Hertz thyratron-switched, transformer-based systems are used. Titan has developed a high-average-power, system capable of very high pulse repetition rates. Among these high voltage sources, Marx generators are well suited for high peak power applications [Miller (1997)].

(b)   Cathode

The injector is basically an explosive emission type cathode which does not require a heater for electron emission. As compared to other explosive emissive materials, velvet is often used in initial devices since it has several beneficial properties,

such as, low electric field threshold, high current density, low plasma closure velocity and inexpensive [Miller (1998)].

(c)   Modulation Cavity

The modulation cavity of the reltron is a side coupled cavity structure, which comprises of two main cavities and a coupling cavity in which coupling cavity is connected to the main cavities through a coupling slot as shown in Fig. 2.1. [Miller *et al.* (1992)]. The main cavities are covered by three grids, placed in the back, middle and front, which allow the electrons to pass through while confining the RF waves in between [Soh (2012)] (Figs. 2.1 and 2.2). The coupling cavity has two idlers which make the re-entrant section of the cavity.

(d)   Post-acceleration gap

The post-acceleration gap is an arrangement of the stacks of alternating plastic insulator rings and aluminium grading rings which act as a high voltage insulator. It lies in between the modulation cavity and RF extraction waveguide. A hollow cone covered with a grid is attached to the output side which is used to shape the electric field in this region thereby reducing the electric field enhancement (Fig. 2.1) [Miller (1996), Soh (2012)].

(e)   Extraction Cavity

Mode converter is a passive device through which EM field profile is converted into another desired EM field profile. It is used in cases, where the RF signal growth in the device occurs in certain particular mode and RF power has to be coupled out and propagated in the external waveguide in its dominant mode.

Since, reltron is a linear beam device, the electron and RF wave interaction should occur in the longitudinal direction. Therefore, in the RF interaction structure the primary operating mode is kept as TM_{01}. Further, in the case of reltron, it is easy to couple out the RF power in the radial direction using a rectangular waveguide in the TE mode (Fig. 2.1). This rectangular output section itself works as a mode converter and an additional external mode converter is not necessary [Miller *et al.* (1992)].

(a) 0-mode   **(b) π/2-mode**   **(c) π-mode**
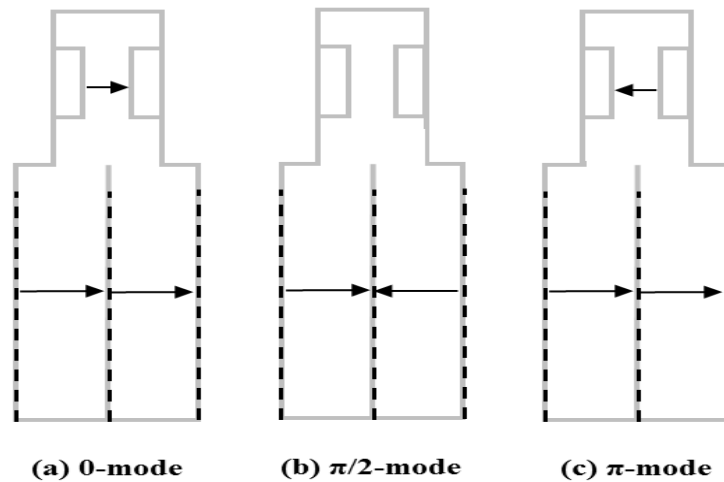
Figure 2.2: Electric field amplitudes of (a) 0-mode, (b) π/2-mode, and (c) π- mode in the side coupled modulation cavity.

2.2.2. Operating Principle

A high voltage pulser is used to provide DC pulsed voltage to the field emissive cathode to produce very high density electrons under the explosive emission condition. The cathode surface contains microprotrusions in the typical size of several tens of microns. Since velvet is a dielectric fibre, the initial electric field in the velvet is equal to the average electric field in the anode cathode gap. When a high DC potential is applied between the cathode and the modulation cavity, the dielectric is polarized and a high electric field at the tip of the microprotrusions is generated. Due to this high electric field, a large negative surface charge density appears on the tip of the

microprotrusions which significantly enhance the local electric field upto 10^4 times. Such field enhancement leads to intense electron field emissions from the microprotrusions with current densities up to 10^6–10^7 A/cm^2. The high current density flowing towards the tip of the whisker leads to fast increase in the temperature of the individual emitters due to *Joule* heating. At this moment, the electron field emission transforms to thermionic electron emission, and the cathode temperature starts increasing. The tip of the whisker can sustain a maximum temperature limit and as this limit is approached; explosion process occurs. Due to this explosion, the cathode material starts vaporising and causes the formation of a neutral cloud which is simultaneously ionized by the electrons, leading to the formation of plasma. The cathode surface is now completely covered by the plasma and acts as a rich source of the electrons. This plasma can provide electron current density up to hundreds of MA/cm^2. The maximum electron current density is limited by the space-charge of the emitted electrons. This process is known as explosive electron emission [Miller (1982), Basu (1995), Barker and Schamiloglu (2001), Krasik *et al.* (2001)].

The modulation cavity operates in the TM_{01} mode, and the radial component of the space charge electric field gets shorted between the metal grid boundaries, and simultaneously it allows the passage of the high current density electrons [Miller *et al.* (1992)]. The self-magnetic field, thus produced focuses the electron beam and eliminates the need for the external DC magnetic focussing field. This phenomenon makes the device compact and lighter in weight. Since the modulation cavity consists of three cavities, three resonant modes can exist inside the cavity, *i.e.*, 0, $\pi/2$ and π modes as shown in Fig. 2.2. From Fig. 2.2, it can simply be inferred that in the 0-mode condition, the electric fields in the main cavities as well as in the coupling cavity are in the same direction. However, in the $\pi/2$ mode, no electric field exists in the coupling

cavity, but in the main cavities, the electric fields are in opposite phase. Whereas in π-mode condition, the electric fields present in the main cavities are in the same phase, but the electric field in the coupling cavity is in opposite phase with that of the main cavities. All the three modes, get excited in the modulation cavity but, only $\pi/2$ mode grows because it is unstable and maximum RF energy transfer only through this mode. Therefore, $\pi/2$ mode is the only mode of operation in case of reltron [Miller *et al.* (1992), Kim *et al.* (2009)]. Principle of the reltron operation is quite similar to that of the klystron except that the electrons undergo double velocity modulation in the modulation cavity causing intense electron bunching [Soh *et al.* (2012)].

A novel concept of an additional post-acceleration region has been introduced in the reltron. Here, the electron beam is first accelerated between the cathode and modulation cavity region and then the bunched electron beam travelling from the modulation cavity towards the RF output cavity is further reaccelerated by applying an additional DC accelerating potential [Hefni (1964)]. This is also known as the voltage stepping [Marder *et al.* (1992)]. Application of this additional accelerating potential causes the electron bunches to pass through the post-acceleration gap with a uniform velocity, approximately equal to the speed of light. Since all the electron bunches have a constant speed, their relative positions are maintained which helps in reducing the relative kinetic energy spread and thus also increases the beam energy [Miller *et al.* (1992)].

The electron bunches passing through the post-acceleration gap are highly relativistic, and power can be extracted from these bunches as they enter the RF extraction cavity. The extraction cavity is a rectangular waveguide through which power can be coupled out directly in its dominant TE_{10} mode [Miller *et al.* (1992), Miller *et al.* (1994)].

2.3. Oscillation Condition

As it can be observed from Fig. 2.1 that the electron beam is pre-modulated at the first grid spacing of the modulation cavity and then enters into the second grid spacing to excite it. As the induced gap voltage in the first grid spacing (between the first and second grids) is high enough, it forms a virtual cathode in the second grid spacing (between the second and third grids). Once the virtual cathode is formed, results into two processes (1) the virtual cathode oscillates in between the first and second grid spacing, and (2) some of the electrons are reflected back towards the cathode, and they are then again reflected back due to the cathode potential towards the virtual cathode. This phenomenon sets up an oscillation in the cavity, known as reflexing [Benford *et al.* (2007)].

The relationship between the induced gap voltage in the first grid spacing and the return current due to the formation of the virtual cathode in the second grid spacing can be obtained with the help of equivalent circuit approach. In this approach, it is assumed that the equivalent series resistance per unit length is R, equivalent series inductance per unit length is L, and the equivalent shunt capacitance per unit length is C. The modulation cavity is represented as a parallel RLC circuit. The circuit inductance and capacitance are related to the resonant frequency by $\omega = (LC)^{-1/2}$ and the quality factor Q can be written as $Q = \omega R C = R / \omega L$. Total current I_t flowing in the circuit is the sum of the currents flowing individually through its circuit elements R, L and C and can be written as:

$$I_t = I_R + I_L + I_C \ .$$

The above expression can be rewritten as:

$$I_t = \frac{V}{R} + \frac{1}{L}\int V dt + C\frac{dV}{dt} \quad .$$

Differentiating the above expression with respect to time t and rearranging the terms

yield:

$$\omega^2 \frac{d^2V}{d\bar{t}^2} + \frac{\omega}{RC}\frac{dV}{d\bar{t}} + \frac{1}{LC}V = \frac{\omega}{C}\frac{dI_t}{d\bar{t}} , \tag{2.1}$$

where $\bar{t}(=\omega t)$ is the normalized time. The total current I_t can now be expressed as

[Uhm *et al.* (1993)]:

$$I_t(\bar{t}) = sI_0 F(\psi,\bar{t}) , \tag{2.2}$$

where I_0 is the initial beam current, s is the form factor which depends on the

geometrical parameters of the cavity, $F(\psi,\bar{t})$ is the normalized beam current at a

location ψ in the first grid spacing and can be given by [Uhm *et al.* (1993)]:

$$F(\psi,\bar{t}) = \frac{\sqrt{1-\psi^2}}{1+\psi\cos\bar{t} + \psi A\{\bar{t}\}\cos(\bar{t} - \varphi\{\bar{t}\} + \alpha)} , \tag{2.3}$$

where $A\{\bar{t}\}$ and $\varphi\{\bar{t}\}$ are the amplitude and phase, respectively, of the induced gap

voltage, in terms of slowly varying function of the normalized time [Uhm (1994)], and

α is the total phase shift due to the return current from the virtual cathode [Uhm (1993)].

Considering $\psi \ll 1$, equation (2.3) becomes:

$$F(\psi,\bar{t}) = 1 - \psi\cos\bar{t} - \psi A\{\bar{t}\}\cos(\bar{t} - \varphi\{\bar{t}\} + \alpha) \quad . \tag{2.4}$$

The total induced gap voltage in the first grid spacing can be obtained from (2.1), (2.2)

and (2.4) as [Uhm (1994)]:

37

$$\frac{d^2V}{d\bar{t}^2} + \frac{1}{Q}\frac{dV}{d\bar{t}} + V = \frac{1}{Q}\phi_w \sin\bar{t} + I_s A\{\bar{t}\}\sin(\bar{t} - \varphi\{\bar{t}\} + \alpha) \ , \tag{2.5}$$

where $\phi_w (= sRI_0\psi)$ is the steady state value to saturate the induced voltage and $I_s (= \omega sI_0\psi/C)$ is the intensity of return current and other coupling mechanism [Uhm (1994)]. Now, the induced gap voltage in the first grid spacing can be expressed in the form [Uhm (1994)]:

$$V\{t\} = A\{\bar{t}\}\sin(\bar{t} - \varphi\{\bar{t}\}) \ . \tag{2.6}$$

The amplitude and phase shift of the induced voltage at the modulation cavity can be given as [Uhm (1993)]:

$$\frac{dA}{d\bar{t}} = \sin\varphi + (h\sin\alpha - 1)A \ , \tag{2.7}$$

and
$$\frac{d\varphi}{d\bar{t}} = \frac{\cos\varphi}{A} + h\cos\alpha \ , \tag{2.8}$$

where the term h is defined for $I_s Q$. Since, $I_s << 1$ and quality factor of the modulation cavity is much larger than unity, the value of h is in order of unity. Further, the values of $A\{\bar{t}\}$ and $\varphi\{\bar{t}\}$ can be obtained by integrating the expressions (2.7) and (2.8), which are nonlinear differential equation and can be solved using fourth order Runge-Kutta method. To solve these equations, it is assumed that the electrons enter the modulation cavity at time $\bar{t} = 0$. The initial conditions for the amplitude and phase are thus given by $A\{0\} = 1$ and $\varphi\{0\} = \pi/2$. This gives a homogeneous solution of amplitude (A), which increases exponentially, provided [Uhm (1994)]:

$$h\sin\alpha > 1 \ . \tag{2.9}$$

This is the self-oscillation condition of the device. As long as, the return current from the virtual cathode is much less than the forward beam current, $I_b \gg I_s$, the modulation cavity is excited linearly. Once the return current becomes significant fraction of the forward beam current, modulation cavity starts saturating, and when the nonlinear saturation condition is considered, expressions (2.7) and (2.8) get modified as [Uhm (1993)]:

$$\frac{d\,A}{d\,\overline{t}} = \sin\varphi + [h(1 - \kappa A^2)\sin\alpha - 1]A, \tag{2.10}$$

and
$$\frac{d\,\varphi}{d\,\overline{t}} = \frac{\cos\varphi}{A} + h(1 - \kappa A^2)\cos\alpha, \tag{2.11}$$

where the nonlinear saturation coefficient $\kappa \ll 1$. When the device parameters satisfy the condition $h\sin\alpha < 1$, the return current damps the induced voltage and the oscillation in the modulation cavity does not sustain. This is an established condition for amplifier operation, typically in the relativistic klystron. However, when $h\sin\alpha > 1$, the amplitude of RF field increases exponentially, which leads to the oscillation condition in the device. The boundary between the amplifier and oscillator condition is $h\sin\alpha = 0$ and under this situation, the electric field amplitude starts saturating. In (2.11), the term κA^2 denotes the saturation amplitude and is given by [Uhm (1994)]:

$$A_s = \sqrt{\frac{h\sin\alpha - 1}{\kappa h\sin\alpha}} \tag{2.12}$$

and $A_s \gg 1$ for self-oscillation condition. The maximum saturation amplitude of reltron can be obtained at the phase angle π/2 because maximum field strength exists in the modulation cavity under the π/2 mode operation.

2.4. Efficiency Analysis

The electronic efficiency of the reltron is obtained by taking the ratio of the average kinetic energy (converted into the RF energy) to the initial electron beam energy. Kinetic energies are calculated by numerically integrating the relativistic electron motion expressions. Reltron uses explosive electron emission condition and to achieve this process, a plasma layer is formed covering the field emissive cathode surface which acts as a rich source of the high current density electrons. The self-magnetic field produced due to the presence of this high density electrons focuses the electron beam, and no external DC magnetic field is required for this purpose. Now, with the presence of electric and magnetic fields, the emitted electrons drift toward the axial direction. The Lorentz force equation in the cylindrical coordinate system, in terms of electron momentum p can be written as:

$$\frac{d\,p}{d\,t} = -e\,(E + v \times B),\tag{2.13}$$

where e and v are the electron charge and velocity, respectively. The self-magnetic field (B) exists in the modulation cavity along with the electric field. It causes the displacement of electrons in the orthogonal direction to the z-axis but, have no effect on the longitudinal direction of motion. Therefore, the effect of self-magnetic field in the axial propagation of electrons is ignored. The RF electric field (E) is generated due to the induced gap voltage $V\{t\}$ inside the modulation cavity which can be approximated by the $\pi/2$ mode of operation as [Miller *et al.* (1992)]:

$$E = \begin{array}{ll} -E_0 \sin(\omega t + \theta) & 0 < z < g \\ E_0 \sin(\omega t + \theta) & g < z < 2g \end{array},\tag{2.14}$$

40

where E_0 is the peak field amplitude, θ is an initial phase condition of the electric field and g is the grid spacing in the modulation cavity (Fig. 2.2(b)) which is given as [Miller *et al.* (1992)]:

$$g = \frac{v_0}{2f} \;\; ,$$

where v_0 is the initial velocity of electrons and f is the resonant frequency. The anode-cathode gap is approximately equal to $1.1g$. In the first grid spacing $0 < z < g$, the force equation can be written as [Soh (2012)]:

$$\frac{dp}{dt} = -eE_0 \sin(\omega t + \theta).$$

Integrating the above expression provides the momentum in the 1st grid spacing, Fig. 2.2(b):

$$\int_{p_0}^{p} dp = -\int_{0}^{t} eE_0 \sin(\omega t + \theta) dt,$$

$$\Rightarrow \quad p(t,\theta) = p_0 \{1 + \varsigma[\cos(\omega t + \theta) - \cos\theta]\}, \tag{2.15}$$

where $\varsigma = eE_0 / \omega p_0$ and p_0 is initial momentum defined by:

$$p_0 = \gamma_0 m v_0, \tag{2.16}$$

where v_0 is the initial velocity of electrons due to the cathode potential. The relativistic mass factor (γ_0) has the form:

$$\gamma_0 = 1 / \sqrt{1 - v_0^2 / c^2}. \tag{2.17}$$

Substituting equation (2.17) in (2.16), the expression for initial momentum can be expressed as:

$$p_0^2 = m^2 c^2 / \sqrt{1 - v_0^2 / c^2} \ .$$

Then, solving the above expression for $(v_0/c)^2$ and substituting it in (2.17) provides γ_0 in the form:

$$\gamma_0 = \sqrt{1 - (p_0 / mc)^2} \ . \tag{2.18}$$

The axial position of electrons can be obtained from (2.16) as:

$$\frac{dz}{dt} = \frac{p_0}{\gamma_0 m} \ .$$

Putting the value of γ_0 in the above expression becomes:

$$\frac{dz}{dt} = \frac{c \, p_0}{\sqrt{m^2 c^2 + p_0^2}} \ . \tag{2.19}$$

Suppose at time $t = T_0$, the electrons enter the second gap, then equation (2.15) at the exit of the first gap gets modified as:

$$p\{T_0, \theta\} = p_0 \left\{ 1 + \varsigma [\cos(\omega T_0 + \theta) - \cos \theta] \right\} \ . \tag{2.20}$$

The force equation in the second grid spacing of the modulation cavity, $g < z < 2g$, can now be written in the form as [Soh (2012)]:

$$\frac{dp}{dt} = e E_0 \sin(\omega t + \theta) \ .$$

Again, integrating the above expression provides the electrons momentum in the 2nd grid spacing as:

$$\int\limits_{p(T_0,\theta)}^{p} dp = \int\limits_{T_0}^{t} eE_0 \sin(\omega t + \theta)dt$$

$$\Rightarrow \quad p\{t,\theta\} = p\{T_0,\theta\} - p_0\varsigma[\cos(\omega t+\theta) - \cos(\omega T_0 + \theta)] . \tag{2.21}$$

Substituting the value of $p\{T_0,\theta\}$ into (2.21) becomes:

$$p\{t,\theta\} = p_0\{1 + \varsigma[2\cos(\omega T_0 + \theta) - \cos(\omega t + \theta) - \cos\theta]\} . \tag{2.22}$$

The above equation gives the momentum of electrons through the side coupled modulation cavity. The normalized electrons momentum after the post-acceleration can be written in the form:

$$\frac{d\overline{p}}{d\overline{t}} = \xi\varsigma[2\cos(\omega T_0 + \theta) - \cos(\overline{t} + \theta) - \cos\theta] \quad , \tag{2.23}$$

where $\xi = V_{pa}/V_{ak}$ is the ratio of post-acceleration voltage to the cathode voltage. The electron trajectory position can be obtained, using (2.23) and (2.19), as:

$$\frac{dz}{dt} = \frac{c\overline{p}}{\sqrt{m^2c^2 - \overline{p}^2}} \quad . \tag{2.24}$$

Reltron is a relativistic device in which the relativistic mass-energy (γmc^2) of the electrons is converted into the RF energy. The initial value of relativistic mass factor γ_0 at the entrance of the modulation cavity, defined by (2.18), gets modified as $\gamma = [1 - (\overline{p}/mc)^2]^{1/2}$. This is the final value of relativistic factor, obtained at the end of the extraction cavity and is also known as Lorentz factor. Using Einstein's mass-energy

equivalence relation, the kinetic energy W_f can be expressed as the difference between the total electron energy and the energy at rest, which is given by [Humphries (1990)]:

$$W_f\{\tau,\theta\} = (\gamma - \gamma_0)mc^2 ,$$

(2.25)

where τ is the total transit time of the electron.

The kinetic energy of the spent beam can be obtained by averaging the electron energies of each electron over the phase angle θ as [Barroso (2004)]:

$$\langle W_B \rangle = \frac{1}{2\pi} \int_0^{2\pi} W_f\{\tau,\theta\} \; d\theta .$$

(2.26)

Now, the electronic efficiency (η) of the reltron is defined as the RF output energy to the DC input electron beam energy. The electronic efficiency of the device can also be estimated as the average loss of the electron energy from their initial value given as:

$$\eta = 1 - \frac{\langle W_B \rangle}{W_{beam}} ,$$

(2.27)

where $W_{beam}(=eV)$ is the total kinetic energy provided by the beam. Here, V $(=V_{ak}+V_{pa})$ is the beam voltage which is the sum of the cathode voltage V_{ak} and post-acceleration voltage V_{pa}. The RF output power of the reltron can be obtained by $P = \eta V I_b$, where I_b is the total beam current.

2.4.   Results and Discussion

Reltron is a relativistic klystron oscillator where the explosive emission process is utilized to produce high current density electron beam. The self-magnetic field of the cavity provides insulation condition and performs vircator action in the modulation

cavity. Starting from the basic principles, expressions for the oscillation condition and electronic conversion efficiency of the device are obtained. In order to validate the analytical approach developed, numerical computations are carried out. The typical reltron device parameters selected as per [Miller *et al.* (1992), Uhm (1994)], for the computations are listed in Table 2.1.

**Table 2.1:** Reltron specifications for the analytical computation

Particulars	Specifications
Frequency (f)	3 GHz
Cathode Voltage (V_{ak})	100 kV
Post-acceleration Voltage (V_{pa})	750 kV
Beam Current (I_b)	750 A
$I_s Q$ Factor (h)	1.5
Saturation coefficient (κ)	0.002

In case of relativistic klystron, the saturation amplitude is known only on the positive side of the phase space for oscillator operation while the steady state value lies on the negative side of the phase space for amplifier operation [Uhm (1993)]. To investigate the behaviour of reltron, a relationship between saturation amplitude (A_s) of the induced gap voltage and phase shift (α) due to the return current from the virtual cathode using expression (2.12) is plotted as Fig. 2.3 (for $h = 1.5$ and $\kappa = 0.002$). From Fig. 2.3, it can be observed that the saturation amplitude (A_s) lies on the positive side of the phase space, which implies that the reltron is working as an oscillator. The range of α for which the saturation amplitude exists is known as the oscillation range of the device. For reltron it lies in between $\pi/4 < \alpha < 3\pi/4$. The oscillation range covers almost

the entire right-hand side of the phase space and closer to $\alpha = \pi/2$, where it has a steeper

growth field amplitude. A comparison of the oscillation range of reltron with relativistic

klystron [Uhm (1994)] is also plotted in Fig 2.3. The oscillation range of such a device

considered in the present work as well as that reported by [Uhm (1994)] is found to be

identical in nature, which proves the validity of the analytical model developed in the
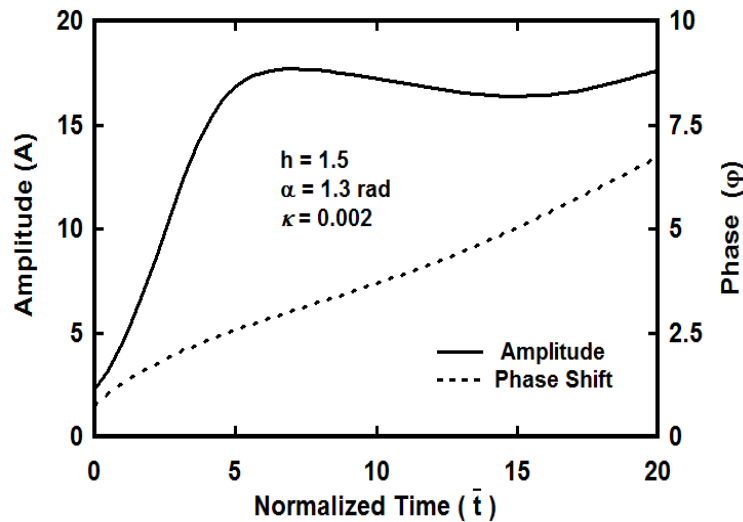
previous section.
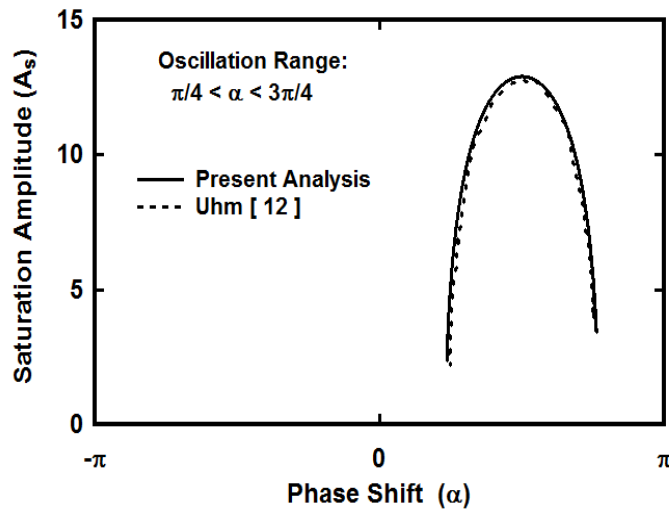
Figure 2.3: Plot of the normalized saturation amplitude (A_s) versus phase shift (α).
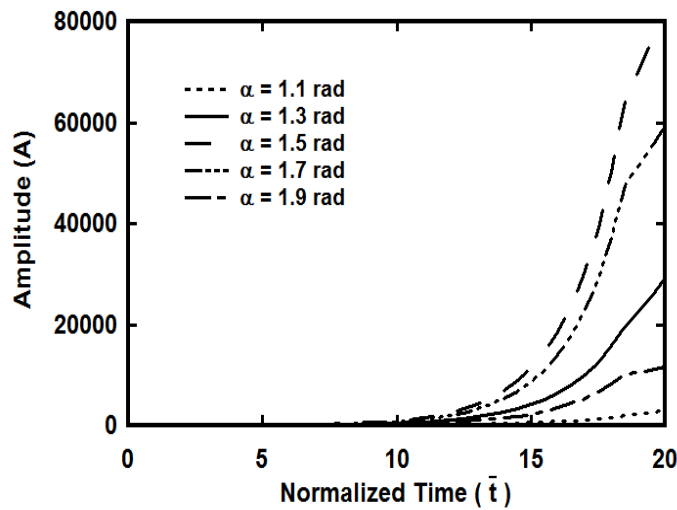
Figure 2.4:   Amplitude of the induced gap voltage of the first grid spacing in the
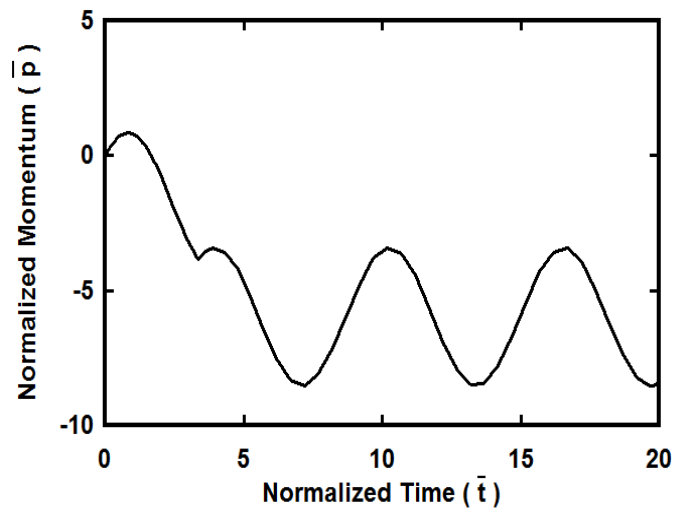modulation cavity versus the normalized time.
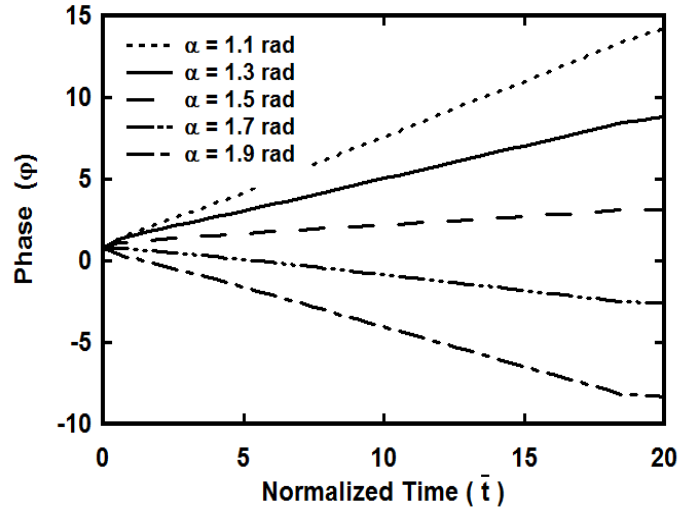
Figure 2.5: Phase of the induced gap voltage of the first grid spacing in the modulation cavity versus normalized time.

Figure 2.6: Amplitude and phase of the induced gap voltage of the first grid spacing in the modulation cavity versus normalized time including the effect of nonlinear saturation.

The amplitude of the induced gap voltage at the first grid spacing in the modulation cavity increases exponentially when the device parameters satisfy the oscillation condition, *i.e.*, $h \sin \alpha > 1$. To study the growth rate of the induced gap voltage with time, expressions (2.7) and (2.8) are solved using fourth order Runge-Kutta

method. The amplitude of the induced gap voltage of the first grid spacing in the modulation cavity is plotted against the normalized time in Fig. 2.4 (for $h = 1.5$ and for different values of the phase shift (α) within the oscillation range). It can be observed that the amplitude exhibits an exponential growth for all values of phase shift angle. At $\alpha = 1.5$ rad, which is near the phase angle $\pi/2$, has a maximum amplitude. From $\alpha = 1.1$ rad to 1.3 rad, the amplitude is in the increasing order, while from $\alpha = 1.7$ rad to 1.9 rad, it is in the decreasing order. Since reltron operates in the $\pi/2$ mode, no field exists in the coupling cavity, and the electric fields in the main cavities are in the opposite polarity, giving a maximum field strength in the modulation cavity [Soh (2012)]. Therefore, phase angle should be kept at $\pi/2$, so that maximum field strength can be obtained.

Figure 2.7: Normalized momentum versus normalized time in the modulation cavity of the reltron.

Further, we have obtained the phase of the induced voltage of the first grid spacing in the modulation cavity using expressions (2.7) and (2.8) and plotted against normalized time. This is shown in Fig. 2.5 at $h = 1.5$ for different values of phase shift within the oscillation range. The phase varies linearly with time, and as the phase shift approaches $\pi/2$, it shows no variation in the induced gap voltage. Furthermore, with the

help of the expression (2.14), it can be observed that the phase angle remained unchanged from first to second grid spacing in the modulation cavity.

To observe the effect of nonlinear saturation, expressions (2.10) and (2.11) are solved using fourth order Runge-Kutta method and the numerical solution for amplitude and phase of the induced gap voltage versus normalized time are plotted in Fig. 2.6. For a typical value of $h = 1.5$, $\alpha = 1.3$ rad and $\kappa = 0.002$, the normalized amplitude increases exponentially in the beginning and then exhibits an oscillation condition, while the phase increases linearly with time.

When the beam current exceeds the space-charge limiting current, the potential is depressed, and the electron beam stops propagating further, which results in the formation of virtual cathode [Benford *et al*. (2007)]. To observe the behaviour of virtual cathode formation, the effect of normalized momentum versus normalized time in the modulation cavity has been plotted in Fig. 2.7 using (2.21). From Fig. 2.7, it can be seen that initially, the normalized momentum is on the positive side, whereas after $\bar{t} = 1.6$ it shifted to the negative side. The shifting of the normalized momentum from the positive to negative indicates the formation of virtual cathode formation in the device. Once the normalized momentum is shifted to the negative side, it continues with the same phase in the remaining span of time, which is just a case of periodic virtual cathode formation.

The electronic efficiency of the reltron is computed using the expression (2.27) for the device parameters listed in Table 2.1 [Miller *et al*. (1992)]. The analytical device efficiency and RF output power are found as ~ 44% and 280 MW at 3 GHz frequency, respectively, whereas   [Miller *et al*. (1992)] experimental device, based on these parameters, yielded an RF output of 235 MW with ~ 37% efficiency.   Further, one more published experimental result for a 3 GHz reltron device [Miller *et al*. (1994)] has

also been considered for the validation. It has been observed that Miller's this experimental device [Miller *et al*. (1994)] produced an RF output power of 350 MW and energy of 40 Joule, while the present analysis exhibits an RF output power of ~ 450 MW and energy equal to 45 Joule for 100 ns pulse duration. Hence, those previously reported experimental values [Miller *et al*. (1992), Miller *et al*. (1994)] are found to be in agreement with the present analytical results within ~ 7-10%.
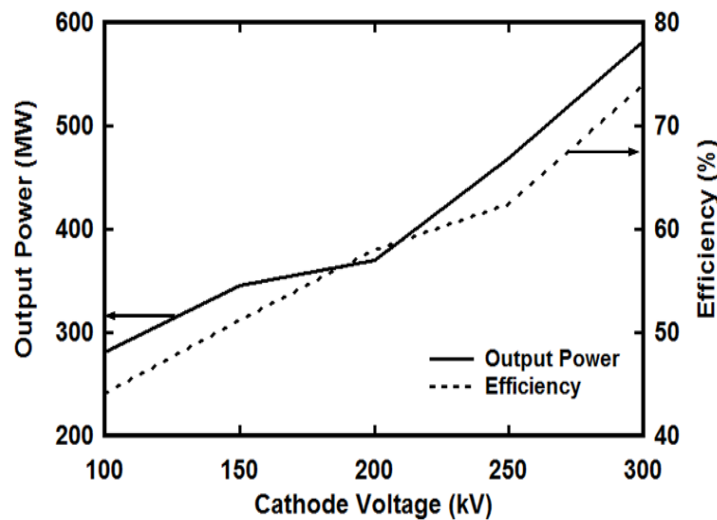
Figure 2.8: RF Output power and efficiency as function of cathode voltage.

The parametric analysis of the reltron is also carried out to study the effect of various device parameters on its performance. The RF output power and efficiency as a function of cathode voltage are plotted in Fig. 2.8 which shows that the parameters for device performance improve with the increase in the applied DC potential. Grid spacing and A-K gap are other important parameters which affect the performance of the reltron. When the A-K gap is smaller than the grid spacing, then the virtual cathode formation does not take place, and for the A-K gap is too large, the current in the modulation cavity becomes very small. Both these conditions deteriorate the device efficiency. The other parameters through which device RF output power and pulse

width can be optimized are the post-acceleration gap and especially the extraction cavity geometry [Miller *et al.* (1992), Miller *et al.* (1994)].

2.5.   Conclusion

A detailed device description and operating principle of the HPM oscillator — reltron have been presented. The oscillation condition of the device has been described. The phase angle for sustained oscillation has been found to lie in between $\pi/4$ to $3\pi/4$ with a peak saturation amplitude at $\pi/2$. The amplitude and phase of the induced gap voltage within the oscillation range have been analysed, and the effect of nonlinear saturation coefficient on these parameters has also been demonstrated. Further, the analytical approach to obtain the electronic efficiency of reltron has been developed. In order to validate the developed analytical approach, comparisons have been made with previously reported experiments results and found, in agreement within ~ 7-10% for RF output power and device efficiency. It is hoped that the present work would be helpful both in the understanding as well as the design and development of the potential HPM oscillator— reltron.